Iranian Journal of Physics Research, Vol. 25, No. 3, 2025
DOI: 10.47176/ijpr.25.3.82159

Improvement of crystallite size, band gap, and electrical conductivity in Cu-doped Co_3O_4 thin films prepared by spray pyrolysis

Sabah Haffas[1], Nadjette Belhamra[*], Okba Belahsen[2], Nourelhouda Redjouh[1], Ferial Belhamra[1], Zahia Bencharef[1]

[1] Physics Laboratory of Thin Layers and Applications, University of Biskra, BP 145 RP, Biskra 07000, Algeria
[2] Laboratory of Metallic and Semi-Conducting Materials, University of Biskra, B.P. 145, 07000 Biskra, Algeria

E-mail: n.belhamra@univ-biskra.dz

(Received 03 August 2025 ; in final form 01 October 2025)

Abstract

In this study, we synthesized undoped and doped cobalt oxide (Co_3O_4) thin films at a concentration of 0.2 M, incorporating varying copper doping levels of 2, 4, 6, 8, and 10 wt. % through spray pyrolysis technique (SPT). The present investigation aims to enhance the characteristics of the films, including the crystalline size, band gap energy, and electrical conductivity. X-ray diffraction patterns (XRD) were used to determine the size of the crystalline structures. The findings indicate that incorporating Cu leads to an increase in the crystallite size. The crystal size (D) increased to 40.94 nm after doping with 10 wt.% Cu. Energy-dispersive X-ray (EDX) mapping analysis validated the presence of copper within the Co_3O_4 thin films. We identified two distinct band gaps from the absorption coefficient measurements: E_1 and E_2. The band gap energy values ranged from 1.441 to 1.388 eV and from 2.061 to 2.012 eV, depending on the Cu doping concentration. The electrical properties demonstrated a reduction in the Rsheet resistance and an enhancement in the electrical conductivity as the concentration of Cu increased.

Keywords: Co_3O_4, Copper doping, structural properties, optical results, Electrical findings.

1. Introduction

Transition metal oxide materials (TMOs) have attracted much attention as promising materials for technological applications due to their electronic, optical and technological properties, such as flexible elemental composition, good ferroelectric properties, adjustable band gaps and catalytic stability [1]. Cobalt oxide is one of the transition metal oxides, and it exists in three structures: CoO, Co_2O_3, and Co_3O_4. CoO rock salt and ordinary spinel Co_3O_4 have stable crystal structures. CoO rapidly oxidizes in the air and transforms into Co_3O_4. Therefore, Co_3O_4 exhibits the highest level of stability [2, 3].

Co_3O_4 has a cubic spinel crystal structure and an excess of oxygen, which gives it p-type semiconductor behavior. It also has a double direct band gap in the visible region of the spectrum, ranging from 2.2 to 1.5 eV [4]. Co_3O_4 classified as a mixed valence antiferromagnetic material. The tetrahedral sites of this material contain a combination of Co^{+2} and Co^{+3}, while its octahedral sites exclusively contain Co^{+3} [5]. Co_3O_4 is a highly effective hole transport layer in solar cells, proving the expertise of materials scientists [6]. Several methods have been used to prepare Co_3O_4 films, including laser deposition [7], the sol-gel method [8], chemical vapour deposition [9], and RF sputtering [10]. Doping of Co_3O_4 thin films has been studied to modify their physical, chemical, electrical, optical, or magnetic properties.

In recent years, studies have shown that doping improves the properties of cobalt oxide (Co_3O_4) thin films. Metal transition has been used as an element-doping method to modify the optical, electrical, and catalytic properties of materials, such as Cu [11], Ni [12], Mn [13], Fe [14], and Zn [15]. Rare earth elements such as Ce [16] and Pb [17] have also been used to change the optical and magnetic properties. Others have shown that non-metal elements, such as P [18], can alter the electronic structure and improve specific properties.

Copper (Cu) doping is commonly used to modify the properties of materials, particularly thin films. When a material is doped with copper, Cu^{2+} ions replace or are incorporated into the crystal lattice of the host material, which can alter its optical, electrical, and structural properties. Doping Co_3O_4 with Cu is a promising method for improving the properties of these films for various applications, including catalysis [19], sensors [20], and electrochemical devices [21]. These studies used cobalt oxide with a spinel structure at a concentration of 0.1 M. This study focuses on enhancing the characteristics of Cu-doped Co_3O_4 thin films.

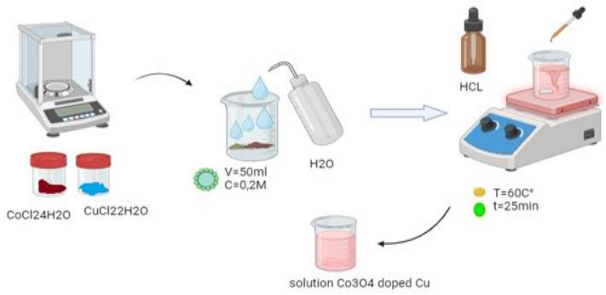

Figure 1. Steps for preparing an undoped and doped Co3O4 solution

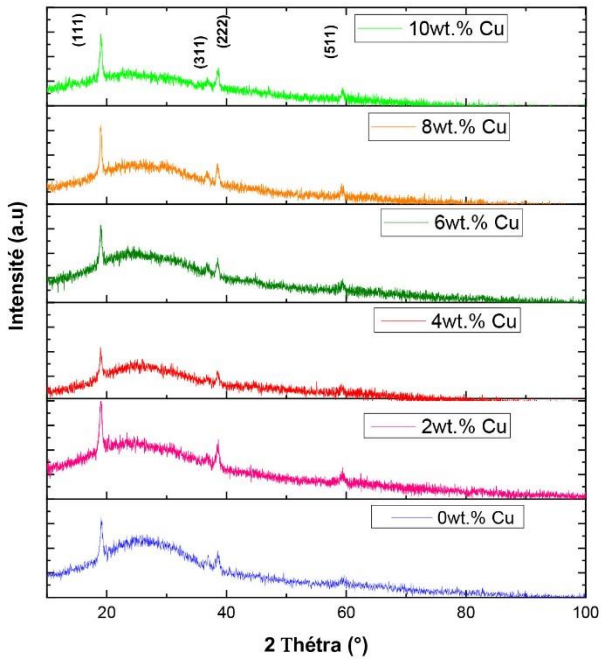

Figure 2. XRD patterns of Cu-doped cobalt oxide (Co_3O_4) thin films at different concentrations.

Table 1. Experimental conditions

Concentration of precursor	0,2 M
Volume of precursor	50 ml
Solvent	distilled water
Spray rate	2 ml/min
Substrate temperature	400 C°
Nozzle substrate distance	10 cm

Using SPT at 400°C, we prepared a solution of cobalt oxide Co_3O_4 with a concentration of 0.2 M. We then proceeded to dope it with varying concentrations of copper and deposited it on the glass substrates. We observed enhancements in various properties, including the crystallite size, band gap, and electrical conductivity. Here is what the remainder of this manuscript is organized as follows.

2. Experimental details

2.1. Materials and deposition of films

To synthesis cobalt oxide (Co_3O_4) thin films, pure and doped, we have used cobalt chloride hexahydrate ($CoCl_2$, $6H_2O$) as a precursor to obtain Co_3O_4, and copper chloride dehydrates ($CuCl_2$, $2H_2O$) as doping, which were added to the precursor solution with different concentrations (0, 2, 4, 6, 8, and 10) wt% (see figure 1). The experiment conditions are illustrated in the Table. 1. Using a spray pyrolysis technique, the obtained solution was applied onto a glass slide with dimensions of 2.5 cm × 1.5 cm × 0.15 cm.

2.2 Characterization of thin films

The structural properties of Cu-doped Co_3O_4 films were analysed by X-ray diffraction (Rigaku type MiniFlex 600) with Cu Kα radiation (λ=0.1541 nm) in the (2θ) range [10-100] and step size 0.02. The film's morphology was observed using a scanning electron microscope (SEM), a mapping technique, and a fluorescence microscope. Optical transmission and absorption spectra were measured in the range (300–1100) using a JASCO V-770 spectrophotometer. The film's electrical properties were measured using four probe points.

3. Results and discussion

3.1. Structural properties

Figure 2 presents the X-ray diffraction (XRD) patterns for cobalt oxide (Co_3O_4) thin films, both undoped and doped with different levels of copper (Cu). The XRD patterns revealed the presence of Miller indices such as (111), (113), (222), and (115). Based on the JCPDS data file n° 98-002-4210, the results indicated the formation of a crystalline phase of cobalt oxide Co_3O_4, characterized by a cubic structure with a spinel-type and Fd3m space group. With increased Cu doping, changes in these peaks might occur due to the substitution of Co atoms by Cu atoms, which can alter the lattice parameters and potentially introduce new phases or defects in the lattice [22], [23]. No copper phase is formed in this study, indicating it was well incorporated. The modification of the crystal structure and the surface morphology due to Cu doping can be quantified by analyzing the peak shifts, intensity changes, and broadening in the XRD peaks. Such analyses provide insights into the crystallite size, strain, and texture coefficient.

Table. 2 presents data on the structural properties of cobalt oxide (Co_3O_4) samples that are undoped and doped with various percentages of copper (Cu).

The crystallite size in the preferential direction (111) was determined using the Debye-Scherrer formula [24]

$$D_{111} = k\lambda/\beta cos\theta \quad (1)$$

D, λ, θ, β and k represent the crystallite size, x-ray wavelength, diffraction peak angle, full width at half maximum and shape factor (0.9), respectively.

The results show that crystallite size increases with the incorporation of copper. The crystal size increased to 40.94 nm when doped with 10% Cu. The results align closely with those of Dalache et al. [25] and Mohd et al. [26]. The observed enhancement in crystalline size corresponding to elevated copper concentration can be ascribed to the substitution of Co ions by Cu ions within the lattice structure, resulting in an enhancement of crystal quality.

Table 2 . Structural parameters of Cu-doped Co_3O_4.

samples	D(nm)	$\varepsilon \times 10^{-3}$	$\delta \times 10^{-3}$ (lines/nm^2)	N(cm^{-2})
undoped	20.47	1.69	2.35	3.36
2 wt.% Cu	25.58	1.35	1.52	1.72
4 wt.% Cu	25.58	1.35	1.52	1.63
6 wt.% Cu	29.29	1.18	1.16	1.11
8 wt.% Cu	34.10	1.01	0.85	0.70
10 wt.% Cu	40.94	0.84	0.59	0.41

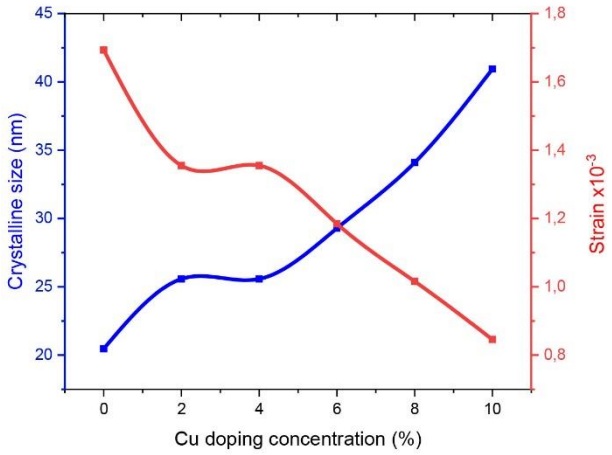

Figure 3. Variation of crystallite size D_{111} and strain ε_{111} of Co_3O_4 thin films as a function of concentrations of copper.

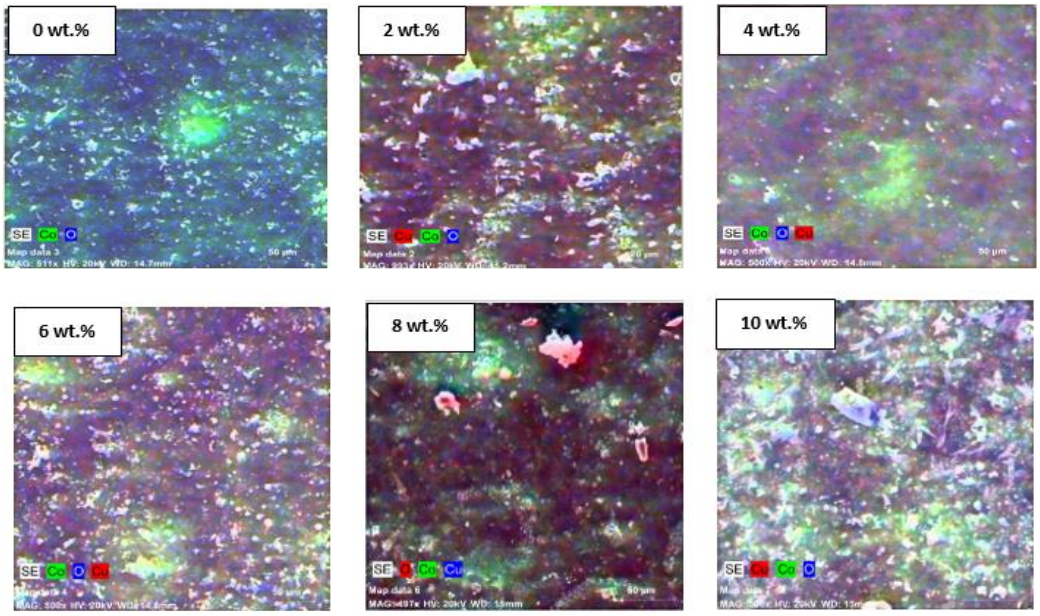

Figure 4. Analysis of elemental distributions in cobalt oxide Co_3O_4 thin films at varying concentrations of Cu doping, as determined through EDX mapping.

The strain (ε) associated with the (111) orientation was determined using the following equation [27]

$$\varepsilon_{111} = \frac{\beta cos\theta}{4} \quad (2)$$

The dislocation density, defined as the length of dislocation lines per unit volume of the crystal, is determined using the relation [28]

$$\delta_{111} = \frac{1}{D^2} \quad (3)$$

The density of crystallites (N), defined as the number of crystallites per unit volume, in Co3O4 thin films is presented in Table 2. The calculation is performed using the following formula [29]

$$N = \frac{d}{D^3} \quad (4)$$

Where d represents the thickness and D denotes the crystallite size.

Obtaining a large crystal size in a sample with a small area indicates a small number of grain boundaries, which leads to a smaller dislocation density and causes a minor strain. This explains the inverse relationship between an increase in crystal size and a decrease in strain (see figure 3). This confirms the reduction in strain mesh due to doping, and the absence of parasitic phases observed for Cu indicates the purity of the prepared samples.

Table 3. EDX data Cu-Co_3O_4 thin films at different concentrations of Cu.

Samples	Co (wt.%)	Cu (wt.%)	O (wt.%)
undoped	7.87	/	56.59
2 wt.% Cu	13.98	0.28	56.22
4 wt.% Cu	8.26	0.38	55.70
6 wt.% Cu	8.91	0.43	60.91
8 wt.% Cu	14.39	1.07	51.72
10 wt.% Cu	21.57	1.86	48.15

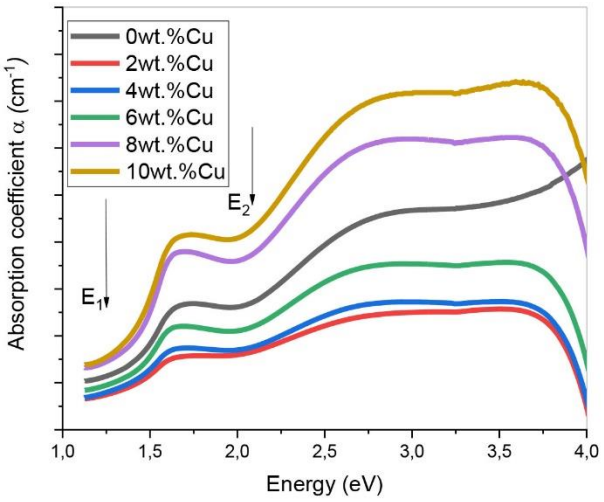

Figure 5. Variation in the absorption coefficient of the undoped and Cu-doped Co_3O_4 thin films with photon energy.

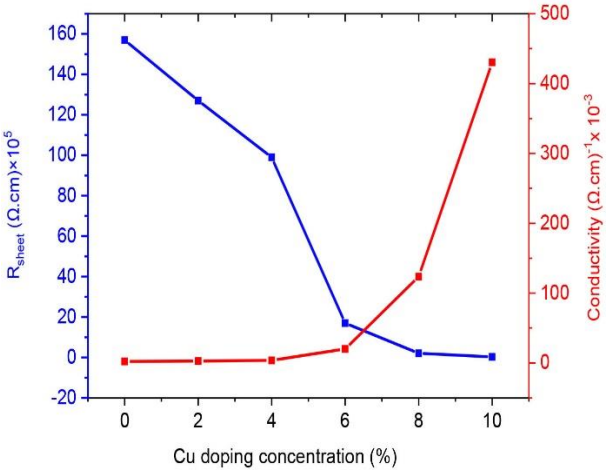

Figure 6. Showcases the variation of the sheet resistance and electrical conductivity of Co_3O_4 with different concentrations of Cu-doping.

3.2. Surface morphology

The incorporation of copper within the cobalt oxide films has been confirmed through EDX-mapping analysis, as illustrated in figure 4, and the elemental chemical compositions presented in Table 3. The atomic percentage of copper increases from 0.28% at 2 wt.% doping to 1.86% at 10 wt.% doping. As the concentration of copper increases, the cobalt content rises correspondingly, increasing from 13.98% at 2 wt.% to 21.57% at 10 wt.%. This suggests a potential mechanism of Co^{+2} ions displacement or substitution under the influence of copper doping [20].

3. 3. Optical properties

Figure 5 represents the absorption coefficient (α) as an energy function for thin films doped with different concentrations of copper (Cu). The absorption coefficient increases as Cu doping concentration increases. The curve for the 10 wt.% Cu-doped sample has the highest absorption over the entire energy range.

All films exhibit two distinct absorption edges within the visible spectrum, a characteristic feature of cobalt oxide films. This phenomenon arises from charge transfer processes, with the initial absorption occurring in the 400 to 500 nm range attributed to the transfer of charge from O^{-2} to Co^{+3}. The second absorption between 700 and 800 nm is observed, resulting from charge transfer from O^{-2} to Co^{+2}. This observation substantiates the existence of two distinct band gap energies, Eg_1 and Eg_2.

The band gap energy was calculated using the Tauc relationship [30]

$$(\alpha h\nu)^2 = A(h\nu - Eg) \quad (5)$$

Where A, hν, Eg and α denote transition constant, photon energy, band gap energy and absorption coefficient, respectively.

The variation of optical band gap of Cu-doped cobalt oxide thin films with different concentrations of Cu values were illustrated in Table 4. The results ranged from 1.441 to 1.388 eV and from 2.061 to 2.012 eV. A reduction in the energy band gap values has been noted; probably due to the creation of receptors within the synthesized gap as Cu cations replace Co cation positions. This displacement leads to a narrowing of the energy gap, consistent with previously reported findings [31]. The emergence of new levels within the band gap results in an upward shift of the valence edge to higher energy levels, consequently reducing the optical band gap values. A reduction in optical properties and band gap can be attributed to increased crystallite size and decreased defect sites. As grain size increases, the density of grain boundaries diminishes, leading to a reduction in carrier scattering at these boundaries. The same findings were observed for Lakhel [13]. Reducing the band gap enhances the conductivity of Co_3O_4 membranes, making them suitable for photovoltaic applications.

3.4. Electrical properties

Figure 6 shows the variation of the resistance R_{sheet} and the electrical conductivity at different concentrations of the dopant Cu.

The sheet resistance (R_{sheet}) is calculated using the following formula [22]

$$R_{sheet} = 4.532\left(\frac{V}{I}\right) \quad (6)$$

Table 4. Band gap energy Values (E_1 and E_2) of cobalt oxide films as a function to Cu-doped concentrations.

Samples	Band gap energy Eg_1 (eV)	Band gap energy Eg_2 (eV)
undoped	1,441	2,061
2 wt.% Cu	1,430	2,030
4 wt.% Cu	1,423	2,027
6 wt.% Cu	1,409	2,024
8 wt.% Cu	1,400	2,021
10 wt.% Cu	1,388	2,012

Table 5. The comparative study of the structural, optical and electrical properties of Cu-doped Co_3O_4 thin films.

Samples	Method used	Experiment conditions	Crystallite size D (nm)	Optical Band Gap Eg (eV) (E_1-E_2)	Electrical Conductivity $\times 10^{-3}$ $(\Omega.cm)^{-1}$	Ref.
0 at. %Cu 2 at. %Cu 4 at. %Cu 6 at. %Cu	Spray pyrolysis	M=0.1 T=450C° t= 20 min Glass substrate	29 27 24 26	2.02 2.00 2.09 1.98	0.43 0.37 0.67 0.35	[34]
0 at. %Cu 2 at. %Cu 4.at.%Cu 6 at. %Cu 8 at. %Cu	Nebulize spray	M=0.1 T=400C° Glass substrate	35 28 10 12	2.11 1.92 1.72 1.86	0.38 2.44 3.12 2.86	[21]
0 wt. %Cu 1 wt. %Cu 3 wt. %Cu 5 wt. %Cu 7 wt. %Cu 9 wt. %Cu	Spray pyrolysis	M=0.1 T=350°C Distance =30 cm Glass substrate	34.92 34.02 30.87 30.81 32.35 34.04	1.48-2.06 1.46-2.04 1.44-2.00 1.42-1.98 1.41-1.96 1.40-1.93	----	[35]
0 wt. %Cu 2 wt. %Cu 4 wt. %Cu 6 wt. %Cu 8 wt. %Cu 10 wt.%Cu	Spray ultrasonic	M=0.2 T=400C° t=5 min Glass substrate	20.47 25.58 25.58 29.29 34.10 40.94	1.44-2.06 1.43-2.03 1.42-2.03 1.41-2.02 1.40-2.02 1.38-2.01	2.20 2.69 3.69 20.04 123.59 430.49	This work

Here, a correction factor of 4,532 is applied to the sample. The film's conductivity (σ) can be calculated using the equation

$$\sigma = \frac{1}{R_{sheet} d} \quad (7)$$

d: is the film's thickness.

From figure 6, we can see a decrease in the sheet resistance R_{sheet} and an increase in the electrical conductivity as Cu-doping increased. This can be due to the rise in the size of the crystallites. The Co_3O_4 thin films prepared by different methods show variations in structural properties that correlate with conductivity levels. Enhanced crystallinity improves electrical performance [32], [22].

Others have demonstrated that doping can significantly enhance conductivity. It was found that manganese-doped Co_3O_4 films had a maximum conductivity of 15.54 S/cm when 6% wt of Mn was added [22]. Adding Fe to Co_3O_4 films also made them more conductor, and the best results were seen at a concentration of 2.5 wt% [33].

The results of the current study concerning the structural, optical, and electrical properties of undoped and Cu-doped Co_3O_4 thin films are summarized in Table 5. It is apparent that we observe good crystallite size, low band gap energy, and excellent electrical conductivity.

4. Conclusion

In this work, undoped and copper-doped cobalt oxide thin films, Cu-Co_3O_4, were deposited on a glass substrate by spray ultrasonic method using cobalt chloride hexahydrate with 0.2 M and copper chloride dehydrate as dopant with different concentrations of Cu-doping (0, 2, 4, 6, 8 and 10) wt.%. The results from X-ray diffraction and energy dispersive spectroscopy mapping validated the successful incorporation of copper within the films.

Adding Cu significantly influenced the structural, optical, and electrical characteristics of Co_3O_4 thin films. The crystalline size increases with higher levels of Cu doping. The energy values for the band gap varied between 1.441 and 1.388 eV and from 2.061 to 2.012 eV, contingent upon the varying concentrations of Cu doping utilized. The electrical characteristics reveal a decrease in the sheet resistance R_{sheet}, coupled with an improvement in electrical conductivity as the concentration of Cu rises.

Aknowledgements

The authors would like to acknowledge to the Pr. Saad Rahmane, Mr. Brahim Gasmi and Pr. Toufik Tibermacine for the support and help.

Authors' contributions

Nadjette Belhamra, Sabah Haffas and Okba Belahsen contributed to the conceptualization of this study. Methodology, formal analysis, data curation, and investigation prepared by all authors. Writing and preparation of original draft by Sabah Haffas, Nourelhouda Redjouh and Ferial Belhamra. Review, writing and editing by Nadjette Belhamra and Zahia Bencharef. Nadjette Belhamra has done the supervision of the manuscript.

References

1. E C Okpara, O C Olatunde, O B Wojuola, and D C Onwudiwe, *Environ. Adv.* **11** (2023) 100341.
2. I Concina and A Vomiero, *Small* **11** (2015) 1744.
3. X Yu, T J Marks, and A Facchetti, *J. Mater. Chem. C* **15** (2016) 383.
4. R Marnadu, M Shakir, J Hakami, I M Ashraf, P Baskaran, D Sivaganesh, K V Chandekar, W K Kim, S Gedi, *Surf. Interfaces* **34**, 102366 (2022).
5. J W Kim, S J Lee, P Biswas, T I Lee, and J M Myoung, *Appl. Surf. Sci.* **406** (2017) 192.
6. Y Zhang, J Ge, B Mahmoudi, S Förster, F Syrowatka, A W Maijenburg, and R Scheer, *ACS Appl. Energy Mater.* **3** (2020) 3755.
7. L Qiao, H Y Xiao, H M Meyer, J N Sun, C M Rouleau, A A Puretzky, D B Geohegan, I N Ivanov, M Yoon, W J Weber, and M D Biegalski, *J. Mater. Chem. C* **1** (2013) 4628.
8. K J Kim and Y R Park, *Solid State Commun.* **127** (2003) 25.
9. D Barreca, C Massignan, S Daolio, M Fabrizio, C Piccirillo, L Armelao, and E Tondello, *Chem. Mater.* **13** (2001) 588.
10. C L Liao, Y H Lee, S T Chang, and K Z Fung, *J. Power Sources* **158** (2006) 1379.
11. M B Muradov, S J Mammadyarova, G M Eyvazova, O O Balayeva, I Hasanova, G Aliyeva, S Z Melikova, and M Abdullayev, *Opt. Mater.* **142** (2023) 114001.
12. Q Cheng, R Zhu, J Zhengzhou, Y Zhang, B Yang, and W Zhang, *J. Alloys Compd.* (2024).
13. L Abdelhak, B Amar, B Bedhiaf, D Cherifa, and B Hadj, *High Temp. Mater. Process.* **38** (2019) 237.
14. P Wei, J Liang, Q Liu, L Xie, X Tong, Y Ren, T Li, Y Luo, N Li, B Tang, A M Asiri, M S Hamdy, Q Kong, Z Wang, and X Sun, *J. Colloid Interface Sci.* **615** (2022) 636.
15. A V Koroleva, A S Ilin, V M Smirnova, N Martyshov, V B Platonov, M N Rumyantseva, A P Forsh, P K Kashkarov, and K Kashkarov, *ChemistrySelect* (2023).
16. G A Babu, G Ravi, T Mahalingam, M Navaneethan, M Arivanandhan, and Y Hayakawa, *J. Phys. Chem. C* **118** (2014).
17. C Schuschke, L Fusek, V Uvarov, M Vorokhta, B Šmíd, V Johánek, Y Lykhach, J Libuda, J Mysliveček, and O Brummel, *Chem. Catal. React. Interfaces* (2021).
18. Z Wang, H Liu, R Ge, R Xiang, J Ren, D Yang, L Zhang, and X Sun, *ACS Catal.* **8**, Issue 3 (2018).
19. J X Flores-Lasluisa, J Quílez-Bermejo, A C Ramírez-Pérez, F Huerta, D Cazorla-Amorós, and E Morallón, *Materials* **12** (2019) 1302.
20. M Zahan and J Podder, *Biointerface Res. Appl. Chem.* **12** (2022) 6321.
21. R Venkatesha, C Ravi Dhasa, R Sivakumar, T Dhandayuthapani, B Subramanian, C Sanjeeviraja, and A M Ezhil Raje, *Solid State Ionics* **334** (2019) 5.
22. Z Bencharef, A Chalaa, R Messemeche, and Y Benkhetta, *Main Group Chem.* **21** (2022) 329.
23. J H Richter, *Digital Comprehensive Summaries of Uppsala Faculty of Science and Technology* **228** (1969).
24. A Abdelkrim, S Rahmane, O Abdelouahab, A Hafida, and N Kabila, *Chin. Phys. B* (2016).
25. C Dalache, H Benhebal, B Benrabah, A Ammari, A Kharroubi, and A Lakhal, *Surf. Rev. Lett.* **26** (2019) 1.
26. M Shkir, *J. Alloys Compd.* **967** (2023) 171637.
27. I B Kherkhachi, A Attaf, H Saidi, A Bouhdjar, H Bendjdidi, Y Benkhetta, R Azizi, and M S Aida, *Optik* **127** (2016) 2266.
28. A Derbali, H Saidi, A Attaf, H Benamra, A Bouhdjer, N Attaf, H Ezzaouia, L Derbali, and M S Aida, *J. Semicond.* **39** (2018) 093001.
29. R D Prabu, S Valanarasu, V Ganesh, M Shkir, S AlFaify, and A Kathalingam, *Surf. Interface Anal.* **50** (2018) 346.
30. R C Ambare, S R Bharadwaj, and B J Lokhande, *Curr. Appl. Phys.* **14** (2014) 1582.
31. A Lakehal, B Benrabah, A Bouaza, C Dalache, and B Hadj, *Chin. J. Phys.* (2018).
32. V V Petrov, V V Sysoev, I O Ignatieva, I A Gulyaeva, M G Volkova, A P Ivanishcheva, S A Khubezhov, Y N Varzarev, and E M Bayan, *Sensors* **23** (2023) 5617.
33. M Manickam, V Ponnuswamy, C Sankar, R Suresh, R Mariappan, A Chandra, and J Chandrasekaran, *J. Mater. Sci. Mater. Electron.* **28** (2017) 18951.
34. M Zahan and J Podder, *Biointerface Res. Appl. Chem.* **12** (2022) 6321
35. I Azhar, H Sahar, and I Maki, *Proc. Int. Conf. TMREES17*, Beirut, Lebanon (2017).